

# Source Model of 11th July, 2004 Zhongba Earthquake Revealed from the Joint Inversion of InSAR and Seismological data

Shengji Wei<sup>1</sup>, Sidao Ni<sup>2</sup>, Xianjie Zha<sup>2</sup>, Zhenjie Wang<sup>2</sup> and Don Helmberger<sup>1</sup>

1, Seismological Laboratory, Division of Geological and Planetary Sciences, Caltech, Pasadena  
2, Earth and Space Science, University of Science and Technology of China, Hefei, China

We use interferometric synthetic aperture radar (InSAR) and broadband seismic waveform data to estimate a source model of the 11th July, 2004 Mw6.2 Zhongba Earthquake, Tibet of China. This event occurred within the seismically active zone of southwestern Tibetan plateau where the east-west thinning of the upper crust is observed. Because of limitations in the existing data set, InSAR data alone cannot determine the area of the fault plane independently of magnitude of slip nor the location of the fault plane independent of the earthquake mechanism. Our seismic data tightly constrain the mechanism and centroid depth of the earthquake but not the horizontal location. Together, two complementary data sets can be used to identify the actual fault plane, better constrain the slip model and event location. We first use regional seismic waveform to estimate point source mechanism then InSAR data is used to obtain better location. Finally, a joint inversion of teleseismic P-waves and InSAR data is performed to obtain a distributed model. Our preferred point source mechanism indicates a moment of  $\sim 2.2 \times 10^{17}$  N·m ( $\sim$ Mw6.2), a mechanism of  $171^\circ$  ( $342^\circ$ )/ $42^\circ$  ( $48^\circ$ )/ $-83^\circ$  ( $-97^\circ$ )/11km, corresponding to strike/dip/rake/depth. The fault plane with strike of  $171^\circ$  and dip of  $42^\circ$  is identified as the actual fault with the help of InSAR data. The preferred source model distributes slips between depth of 5~11km and 10km along strike with maximum slip amplitude of about 1.5m.

## Joint Inversion for finite slip model

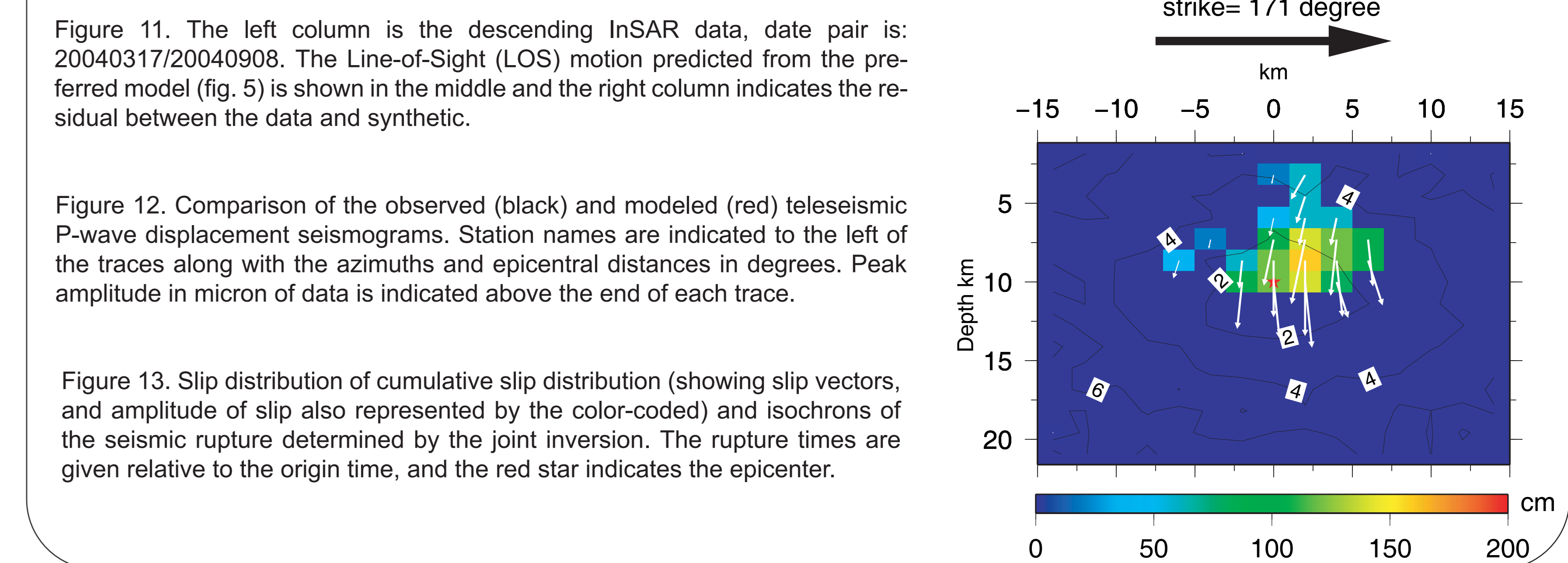
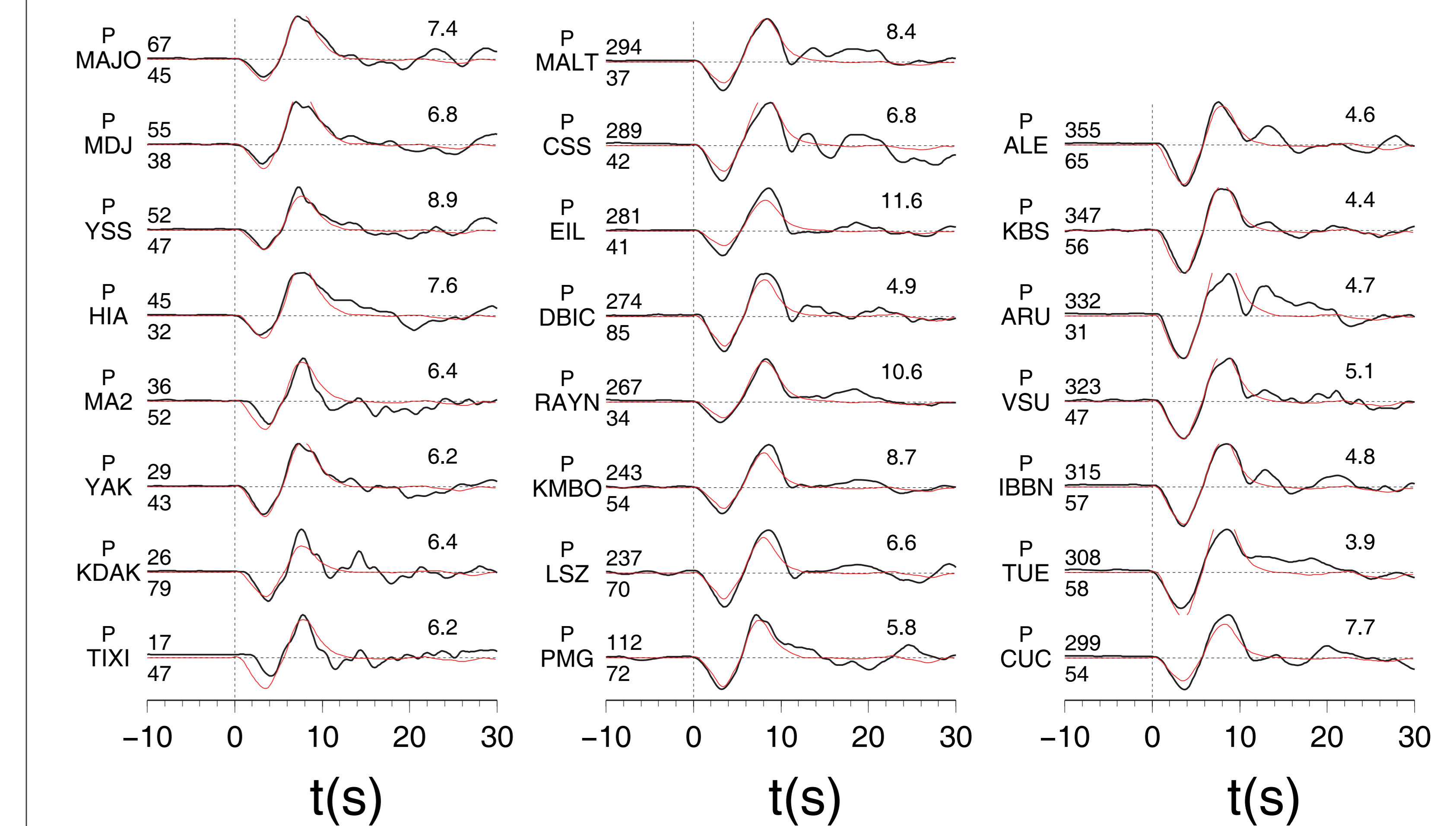
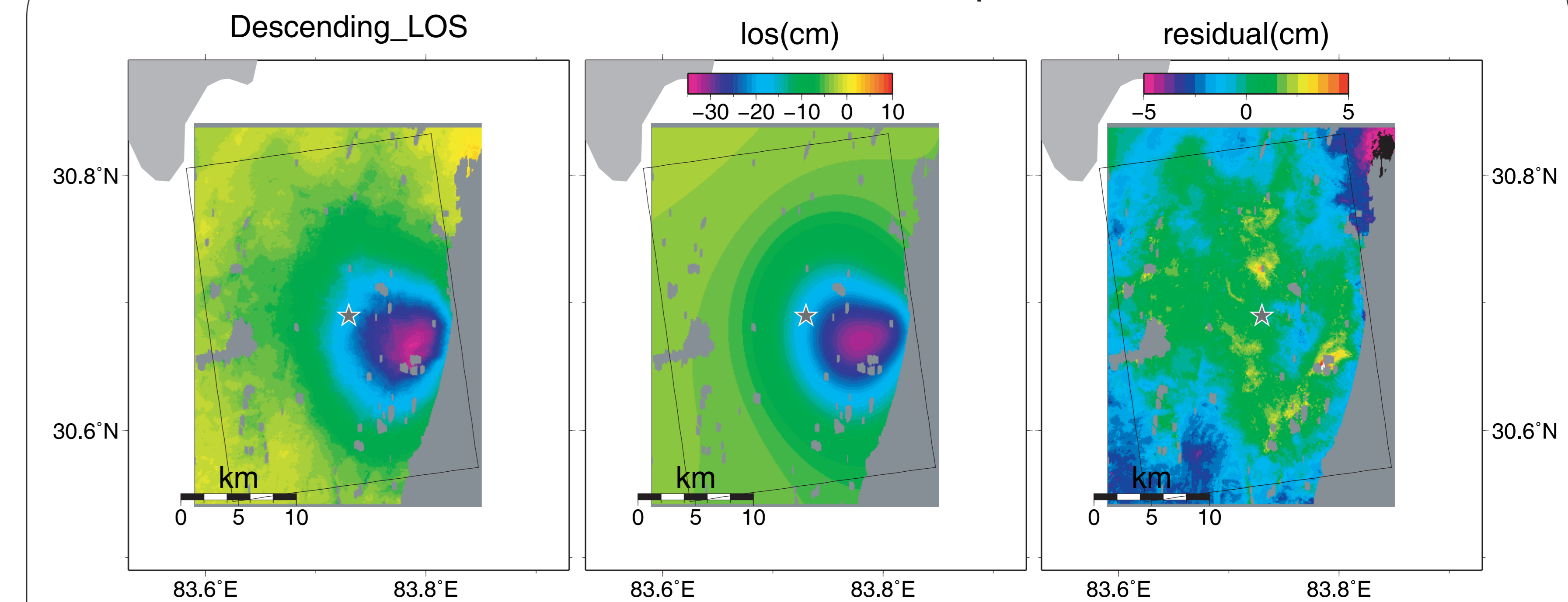


Figure 11. The left column is the descending InSAR data, date pair is: 20040317/20040908. The Line-of-Sight (LOS) motion predicted from the preferred model (Fig. 5) is shown in the middle and the right column indicates the residual between the data and synthetic.

Figure 12. Comparison of the observed (black) and modeled (red) teleseismic P-wave displacement seismograms. Station names are indicated to the left of the traces along with the azimuths and epicentral distances in degrees. Peak amplitude in micron of data is indicated above the end of each trace.

Figure 13. Slip distribution of cumulative slip distribution (showing slip vectors, and amplitude of slip also represented by the color-coded) and isochrons of the seismic rupture determined by the joint inversion. The rupture times are given relative to the origin time, and the red star indicates the epicenter.

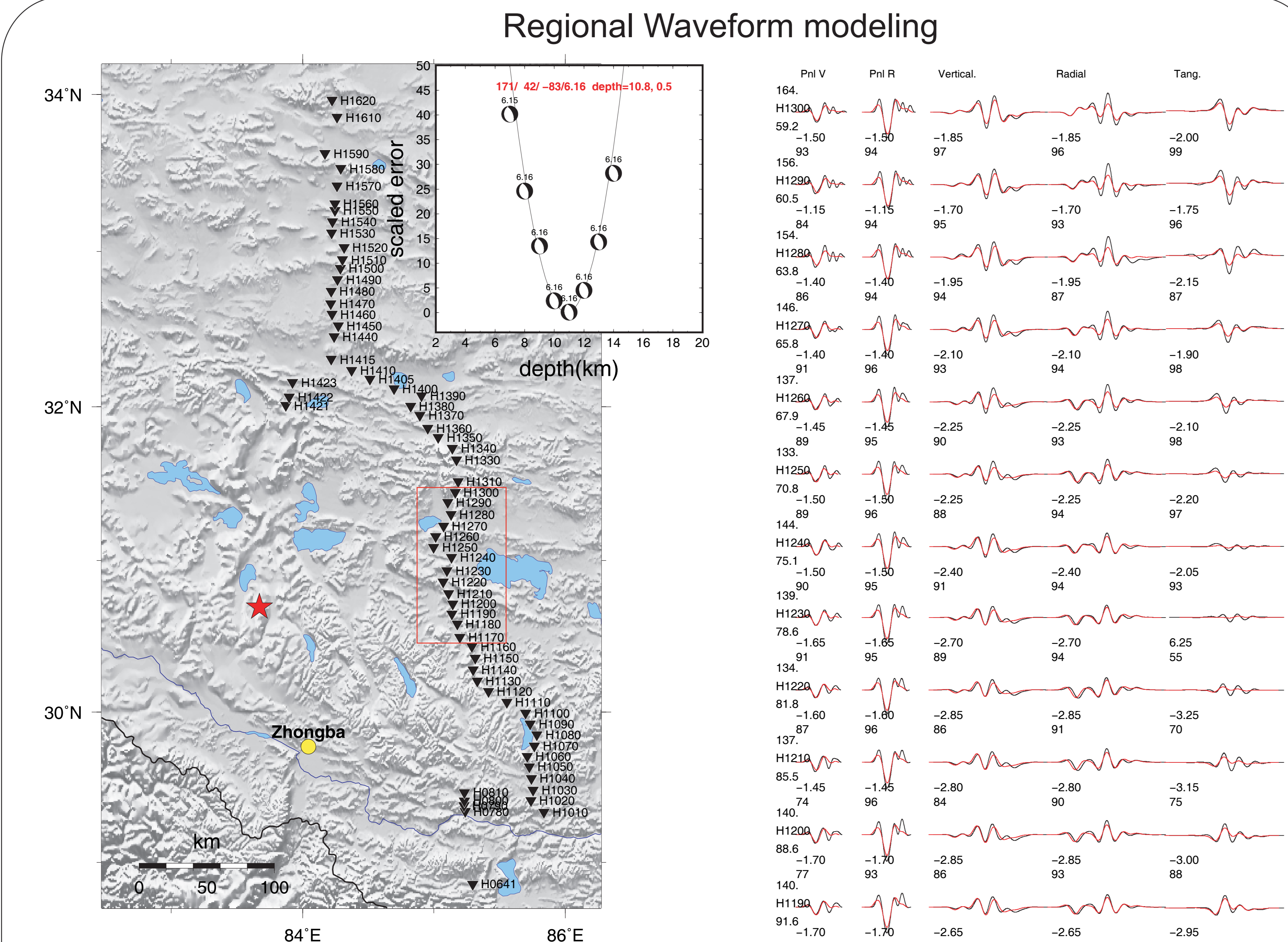


Figure 1. Regional (left) and teleseismic (right) broadband stations (triangles) used in this study for the July 11th, 2004 Zhongba Earthquake in western Tibet of China, the stars indicate the epicenter and the yellow circle is the Zhongba County. Depth resolution of the Cut-And-Paste (CAP) inversion for the July 11th, 2004 Zhongba Earthquake, the point source mechanism we obtain is  $171^\circ/42^\circ/-83^\circ/6.16/11$ km (strike /dip /rake /moment magnitude/depth).

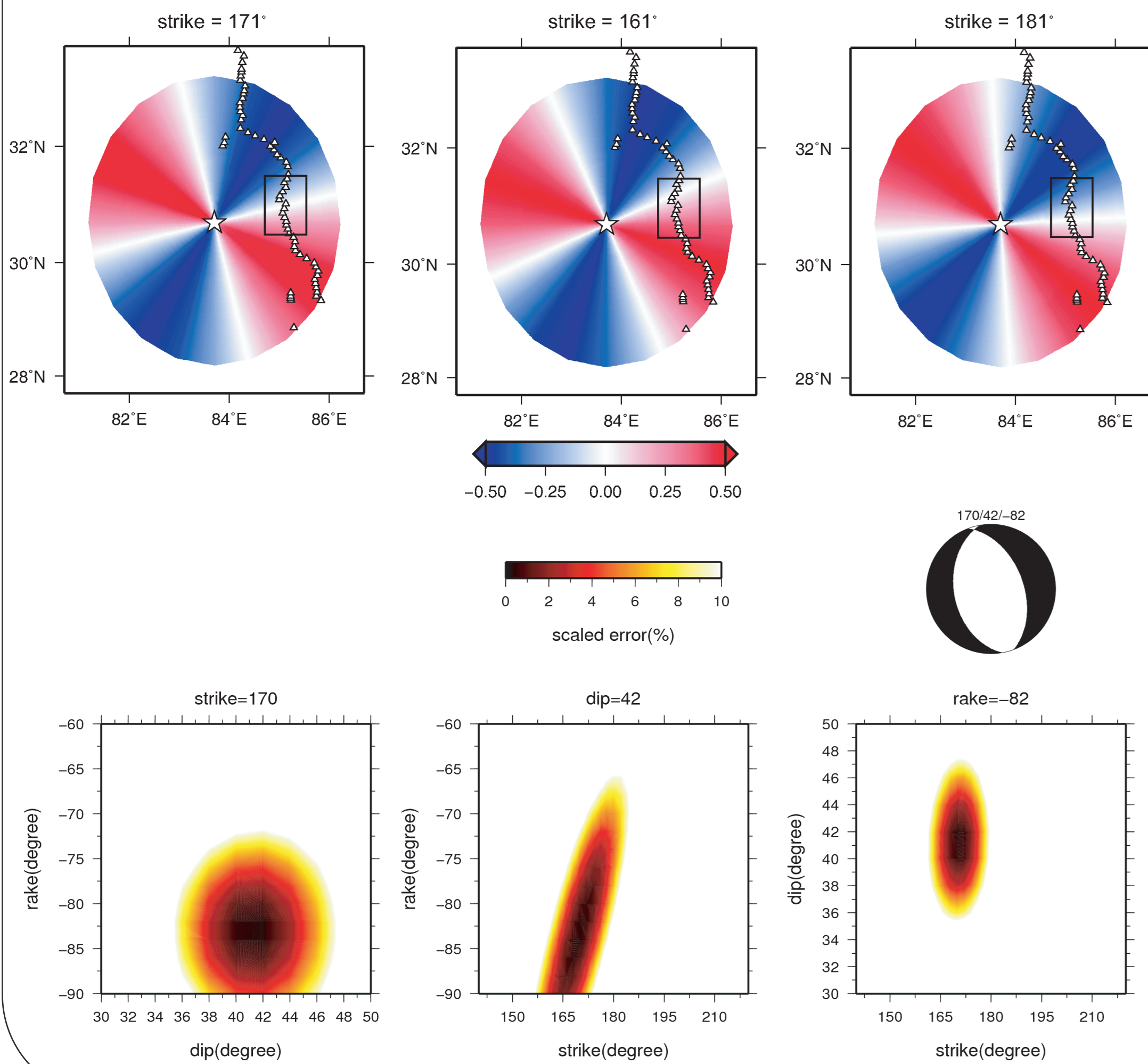


Figure 2. Regional displacement of data (black) and synthetic (red) calculated by the best point source mechanism (see Fig.1 for the mechanism). Waveforms at each station are broken into Pnl (vertical and radial) waves and surface waves (vertical, radial and tangential). Station name is indicated at the left side of each wave train, with epicenter distance above (in km) and azimuth below (in degree). The first number below every waveform pair is the time shift necessary to align them up and the second number is cross-correlation coefficient in percentage. Pnl waves are filtered between 5~50 sec and surface waves are filtered between 10~100 sec. Here we show only a portion of fits to data on which we can see clearly the nodal direction of SH wave radiation pattern.

Figure 3. Normalized radiation pattern of direct SH waves for strike of  $171^\circ$  (left),  $161^\circ$  (middle) and  $181^\circ$  (right), while dip( $42^\circ$ ) and rake( $-83^\circ$ ) angles are fixed. White triangles are regional broadband stations, the small black box indicates the stations used in Fig.1. Epicenter of the earthquake is shown as white star.

Figure 4. Resolution of strike, dip and rake for regional waveform inversion, colored by the scaled misfit errors. The best point source mechanism is  $171/42/-83$ .

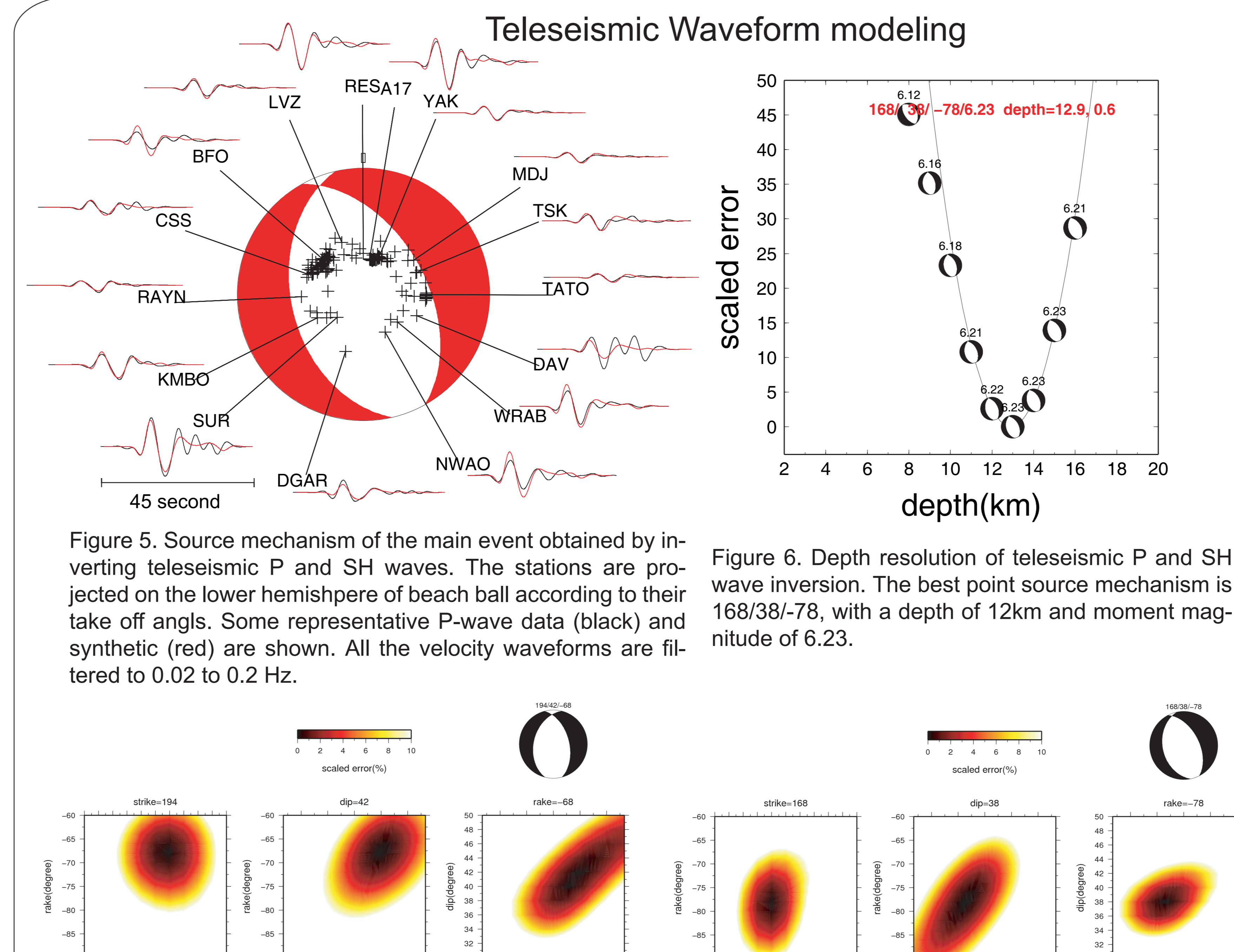


Figure 5. Source mechanism of the main event obtained by inverting teleseismic P and SH waves. The stations are projected on the lower hemisphere of beach ball according to their take off angles. Some representative P-wave data (black) and synthetic (red) are shown. All the velocity waveforms are filtered to 0.02 to 0.2 Hz.

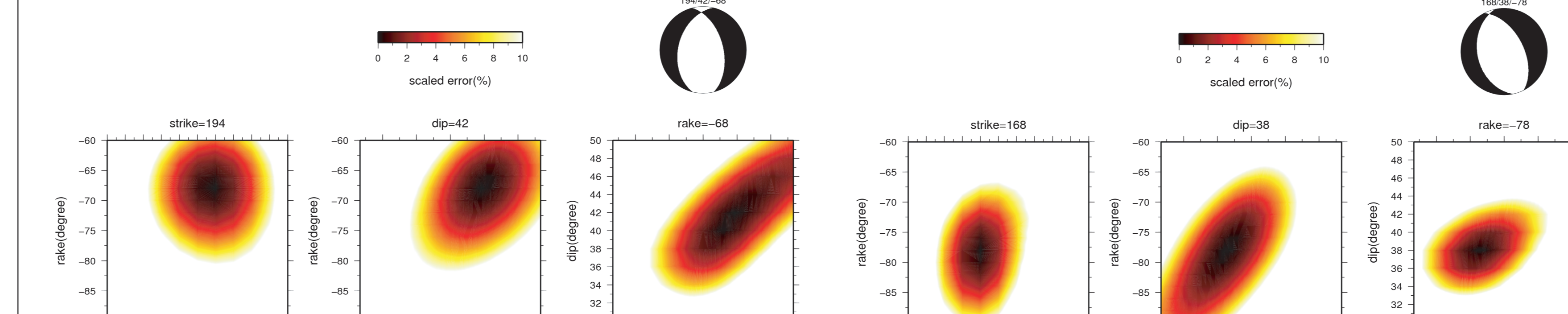


Figure 6. Similar as Fig.7 but for teleseismic P and SH wave inversion, the best point source mechanism is  $168^\circ/38^\circ/-78^\circ$ .

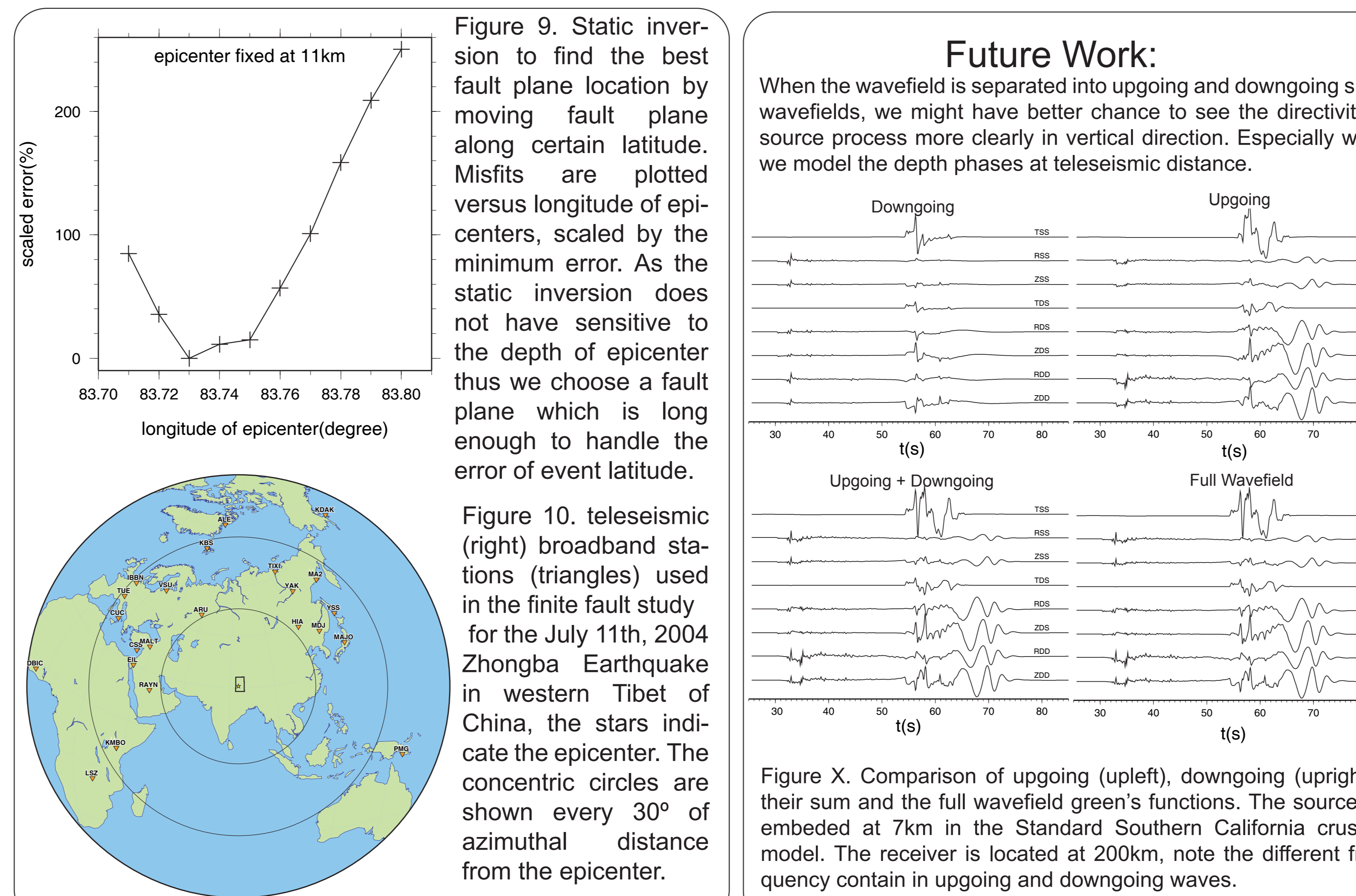


Figure 7. Resolution of strike, dip and rake for teleseismic P-wave only inversion, colored by the scaled misfit errors. The best point source mechanism is  $194^\circ/42^\circ/-68^\circ$ .

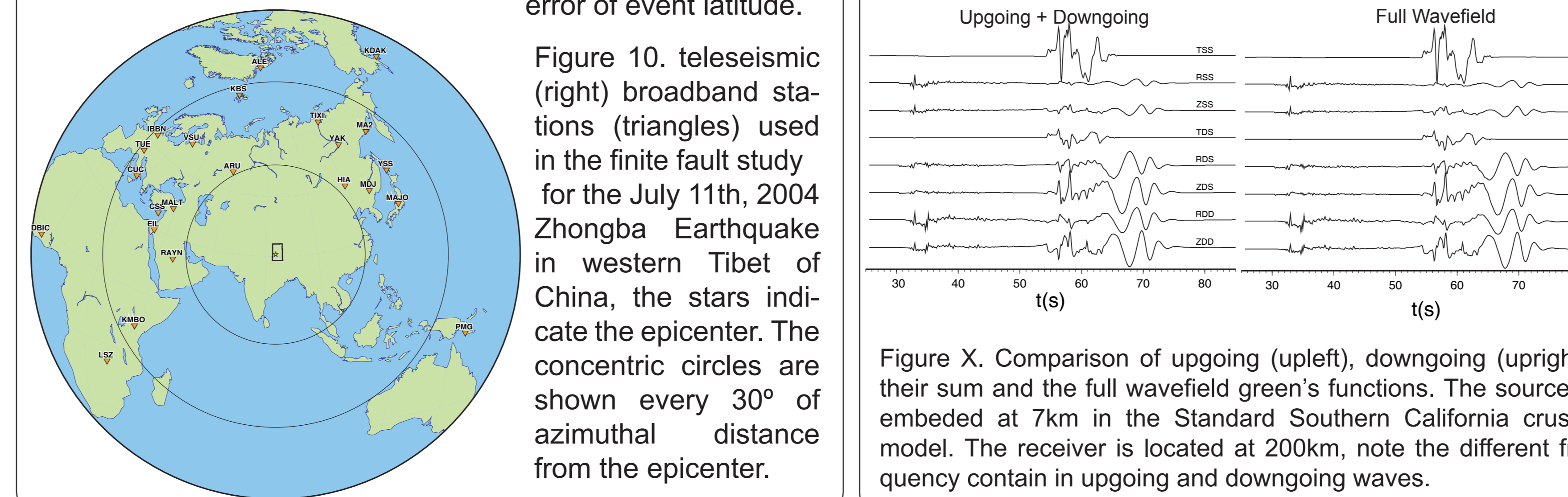
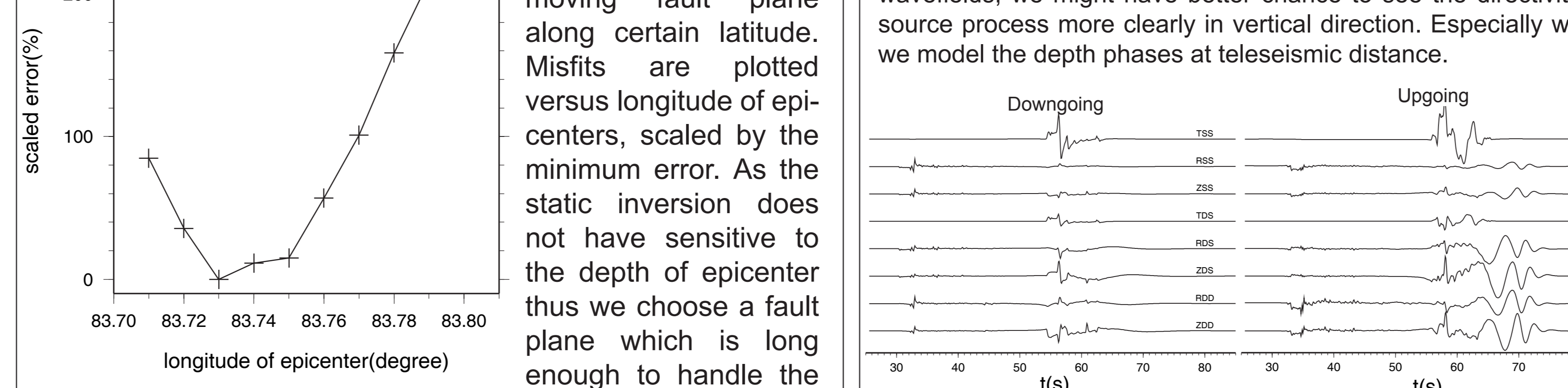


Figure 8. Static inversion to find the best fault plane location by moving fault plane along certain latitude. Misfits are plotted versus longitude of epicenters, scaled by the minimum error. As the static inversion does not have sensitive to the depth of epicenter thus we choose a fault plane which is long enough to handle the error of event latitude.

Figure 9. teleseismic (right) broadband stations used in the finite fault study for the July 11th, 2004 Zhongba Earthquake in western Tibet of China, the stars indicate the epicenter. The concentric circles are shown every  $30^\circ$  of azimuthal distance from the epicenter.

## Future Work:

When the wavefield is separated into upgoing and downgoing sub-wavefields, we might have better chance to see the directivity of source process more clearly in vertical direction. Especially when we model the depth phases at teleseismic distance.

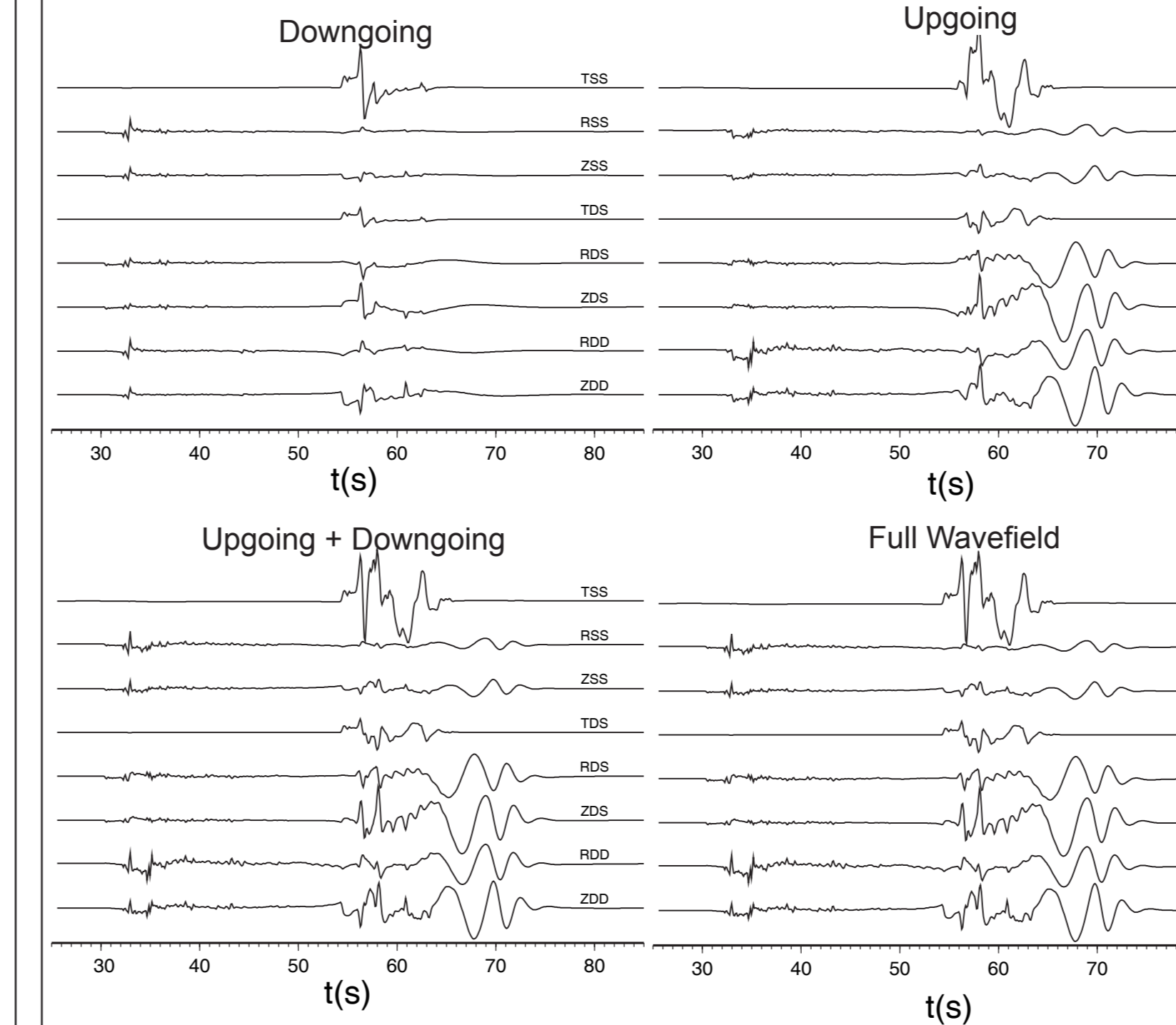


Figure 10. Comparison of upgoing (upleft), downgoing (upright), their sum and the full wavefield green's functions. The source is embedded at 7km in the Standard Southern California crustal model. The receiver is located at 200km, note the different frequency contain in upgoing and downgoing waves.

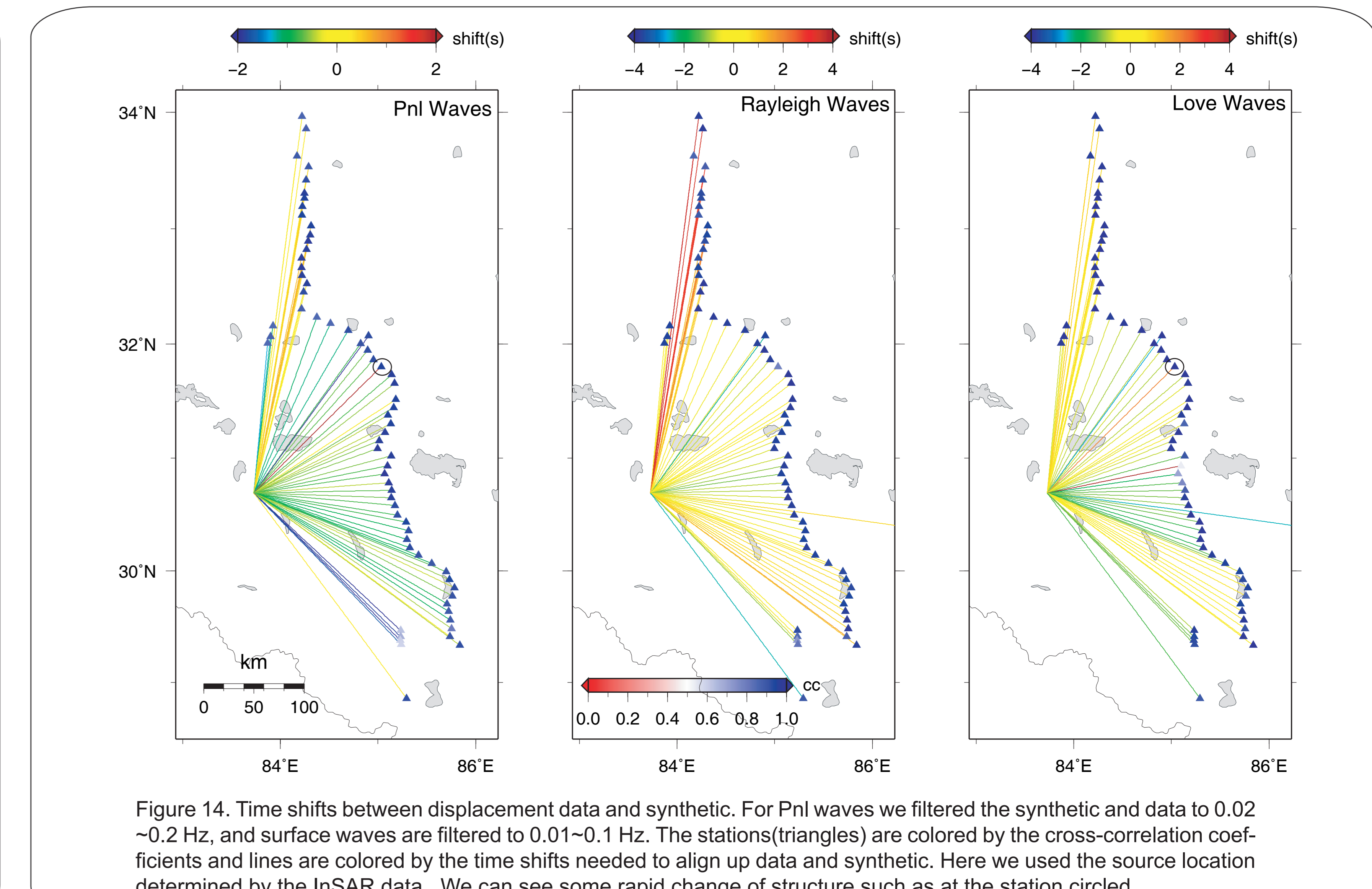


Figure 14. Time shifts between displacement data and synthetic. For Pnl waves we filtered the synthetic and data to 0.02~0.2 Hz, and surface waves are filtered to 0.01~0.1 Hz. The stations (triangles) are colored by the cross-correlation coefficients and lines are colored by the time shifts needed to align up data and synthetic. Here we used the source location determined by the InSAR data. We can see some rapid change of structure such as at the station circled.